TIME VARIATION OF THE X-RAY SPECTRUM AND OPTICAL LUMINOSITY OF SCO X-1

T. KITAMURA*, M. MATSUOKA, S. MIYAMOTO, M. NAKAGAWA*, M. ODA, Y. OGAWARA and K. TAKAGISHI*

Institute of Space and Aeronautical Science, University of Tokyo, Tokyo, Japan

and

U. R. RAO, E. V. CHITNIS, U. B. JAYANTHI, A. S. PRAKASA-RAO and S. M. BHANDARI

Physical Research Laboratory, Ahmedabad, India

(Received 22 March, 1971)

Abstract. Results of rocket observations of SCO X-1 over the spectral range of $2 \sim 20$ keV are presented. The observations have been performed partly in India and partly in Japan under the collaboration of the three groups. The present results are compared with results of similar observations carried out by the LRL (Lawrence Radiation Laboratory) group. Some of these X-ray observations were accompanied by simultaneous optical observations. Relationships between the hardness of the X-ray spectrum and the X-ray intensity and between the hardness and the optical luminosity are compiled. The relationships among the parameters (temperature, density and size) which characterize the postulated isothermal cloud model of SCO X-1 are given. They indicate that SCO X-1 is characterized by a temperature of about 10^7–10^8 K, a density of about 10^{16}–10^{17} cm^{-3} and a radius of about 10^8–10^9 cm respectively. We further show that the temperature is inversely correlated with the size of the source; an increase in temperature corresponds to a decrease in the radius and an increase in density.

1. Introduction

Since the discovery of SCO X-1 by Giacconi *et al.* (1962), a number of observations have been performed to determine its location, flux and energy spectrum. The X-ray observations have indicated that the energy spectrum of the SCO X-1 X-ray source in the energy range 2–20 keV exhibits apparent time variations. After the optical identification of SCO X-1 by Sandage *et al.* (1966), Hiltner and Mook (1970) and others have carried out systematic and extensive photometric observations through 1967–1969 to investigate the time variation of its optical luminosity. These observations have clearly revealed that the optical intensity of SCO X-1 represented by the blue magnitude, B, varies between 12.5 mag. and 13.4 mag. within a few hours.

The purpose of the present observations was to acquire observational data on SCO X-1 for a systematic study of its variation. A series of observations were organized as a part of the collaboration between the Physical Research Laboratory, Ahmedabad, India (PRL), the Institute of Space and Aeronautical Science, (ISAS) and the Osaka City University, Japan, partially supported by NASA, U.S.A. Under this program, a number of rocket launchings were carried out from both India and Japan using essentially similar X-ray payloads and aspect sensors. Extreme care was taken in all

* Department of Physics, Osaka City University, Osaka, Japan.

Astrophysics and Space Science **12** (1971) 378–393.

these measurements to ensure accurate calibration to be able to derive the absolute flux of X-rays with good accuracy. In this paper we report the results of four such rocket observations, two of them carried out on April 26 and 28, 1969 from the Thumba Equatorial Rocket Launching Station (TERLS), India (8°32′N; 76°51′E) and the other two performed on August 7 and 8, 1969 from the Kagoshima Space Center (KSC), Japan (31°15′N; 131°04′E).

Since technical details and methods of analysis appear to be similar to those of the observations performed by the LRL group (Burginyon *et al.*, 1970), we consider it safe to compare the results. Some of the observations were accompanied by simultaneous optical observations.

An isothermal hot cloud model which may be characterized by its temperature, density and size was postulated for SCO X-1. The energy spectrum in the range 2–20 keV for each X-ray observation has been fitted to the free–free emission spectrum of a hot thin plasma. An attempt is made to fit the observations to a free–free emission spectrum which is represented by the temperature of the hot plasma, T, and $n^2r^3/3d^2$, where n is the electron density of the source, r the radius of the source and d is the distance from the Earth to the source.

Observations of Neugebauer *et al.* (1969) suggest that the SCO X-1 source is semi-opaque in the optical and near-infrared regions. A comparison between the observed optical intensity, corrected for the interstellar absorption, and the free–free emission spectrum of the hot plasma as determined by the X-ray observation, yields an estimate of n^2r. Simultaneous X-ray and optical observations thus determine T, $n^2r^3/3d^2$ and n^2r, and accordingly a combination of T, n and r which characterize an isothermal hot cloud. Since the electron scattering of photons in the cloud may distort the spectrum, we also discuss this effect (Loh and Garmire, 1970).

Recently results of satellite observations of SCO X-1 during periods containing optical flaring and sudden increases of the X-ray intensity have been reported (Hudson *et al.*, 1970; Evans *et al.*, 1970). The published results are plotted in our diagrams representing the correlations between $n^2r^3/3d^2$ versus kT and B versus kT. The satellite results show that in the flare phase the relation between T and $n^2r^3/3d^2$ is different from that in the non-flare (quiet) phase. We interpret the results as showing that most of the rocket observations, if not all, which we describe in this paper were performed while the source was quiet.

2. TERLS Experiment

The X-ray payload in the two flights conducted from TERLS consisted of two identical proportional counters, back to back, each of effective path length of 26 mm and effective area of 55.4 cm^2. The counters were filled with 655 Torr of Xe and 65 Torr of methane and had a beryllium entrance window of 115 ± 15 μ thickness. The counter were mounted with their long side parallel to the axis of the rocket which was launched almost vertically to enable the detector to scan all the sources in the horizon of the rocket. Slats type, photo-etched collimators, having half widths of transmission of

32.5° in the longitudinal axis of the rocket and of 10.5° in the azimuthal direction of the rocket, were used to define the geometrical sensitivity of the counters.

The counters had a typical energy resolution of 22% full width at half maximum at 5.9 keV (^{55}Fe) and 15% full width at half maximum at 22 keV (^{109}Cd).

Output pulses from the counters were amplified, shaped and pulse-height-analysed in the energy range 2∼18 keV into five energy windows of nominal values 2–4, 4–6, 6–8, 8–14, and 14–18 keV. Entire information was telemetered by an FM/FM telemetry system. Monitoring of the 5.9 keV line from the ^{55}Fe radioactive source, mounted on the inside of the split nose-cone of the rocket, provided inflight calibration upto 60 km altitude, at which the source along with the nose-cone was explosively ejected.

The two sets of X-ray payloads on board Nike-Apache Rockets (flights 40.04 and 40.05) were launched for TERLS at 1700 UT on April 26, 1969 and 1704 UT on April 28, 1969, respectively. Both rockets were spin-stabilized at about 6 rps and reached an apogee of about 150 km. Useful data were obtained for nearly 200 s from each of these two flights.

3. KSC Experiment

The X-ray detectors launched from KSC also consisted of two identical proportional counters (counter *A* and counter *B*). The counters were filled with 300 Torr Xe and 10% methane gas and were equipped with 108 μ beryllium windows of 38 cm^2. The thickness of the window of each counter was compensated with thin mylar film to make it uniform and equal to one another. The counters had a typical resolutions of 22% for 5.9 keV X-rays. The calculated efficiency curve of each counter was checked with K X-rays of A1, S, Cu and Ag. The stability of the system throughout the flight was monitored with an ^{55}Fe X-ray source introduced into the field of view of the detector once every 36 s.

The field of view of each counter as limited by a slats collimator was 7° FWHM in the azimuth and extended from −13° to +55° in the elevation of the rocket frame of reference. The long direction of the field of view of counter *A* was parallel to the rocket spin-axis and that of counter *B* was slanted by 25°. The time and the amplitude of each pulse produced in the counters were telemetered to the ground.

The first flight from KSC used Kappa-9M-27 rocket, which was launched at 1215 UT on August 7, 1969. It was spin-stabilized at approximately 2 rps. The rocket reached an apogee of about 330 km. During the flight X-ray observations were performed for approximately 500 s. The second observation from KSC was conducted using S-210-2 rocket, which was launched at 1200 UT on August 8, 1969. Its spin rate was approximately 2 rps and reached an apogee of about 101 km.

4. Method of Analysis

The angular motion of a freely spinning rocket is basically composed of a spin motion and a precession. The peak to peak amplitude variation of the horizontal magnetic

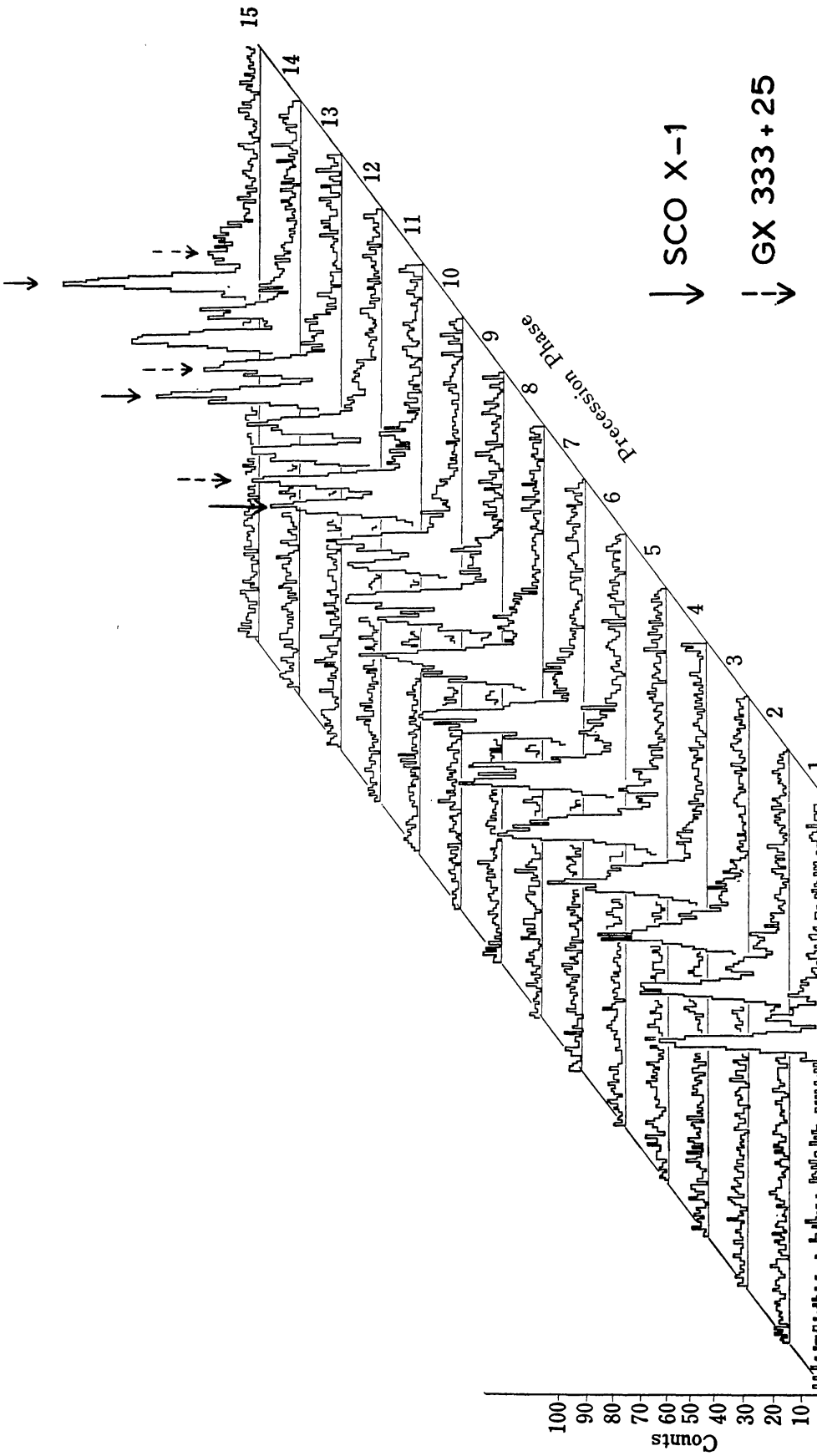

Fig. 1. The counting rate as a function of rocket azimuth during different precession phases for the flight conducted from KSC on August 7, 1969.

sensor and the variation of the vertical magnetic sensor produce approximate values for the spin period and the precession half cone angle. After determining the approximate spin period the precession-spin-phase diagrams of X-ray counts (i.e. the plot of X-ray counts against the spin and precession phases) and of magnetic records were drawn, adjusting the spin period to achieve synchronization of phase of the magnetic record as well as the X-ray pulses from SCO X-1 during different phases of the precession period. A typical example of a spin phase diagram is shown in Figure 1. The two conspicuous peaks marked in the spin phase diagram plotted in Figure 1 correspond to the flux from SCO X-1 and the newborn X-ray source GX 333+25 (Conner *et al.*, 1969; Kitamura *et al.*, 1969).

The angle between the precession axis and the geomagnetic line of force, and the coning angle of the precession was obtained by means of the geomagnetic aspectometer. The angle between the precession axis and the direction of SCO X-1, and also the coning angle, were obtained by the analysis of relative azimuthal phases of SCO X-1 acquisition by counter *A* and *B*. The precession axis was determined to one of the intersections of two small circles centered at the magnetic line of force and SCO X-1 respectively. One of these two intersections was then chosen with the aid of the knowledge of the rocket trajectory. The aspect of the rocket was thus determined with an accuracy of approximately one degree throughout the flight above 90 km. Table I gives the particulars of all four rocket flights.

Figure 2 shows the counting rate as a function of azimuth in 2 to 6 keV energy bands for both the TERLS flights (40.04 and 40.05). Besides SCO X-1 there are many other sources in the region of the galactic centre which also contribute to the counting rate. The contributions due to all the sources to the counting rate during different precession phases have been estimated and used to correct the observed data to obtain the actual counting rate due to SCO X-1, when corrections were necessary. The energy

TABLE I

Data of four rocket flights

Flight No.	Time	Zenith coordinates		Precession axis		Half cone precession angle
		RA	Declination	RA	Declination	
TERLS, India						
40.04	1700 UT 26 April, 1969	12^h26^m	8°33′	177° ± 1°	6°30′ ± 1°	6° ± 2°
40.05	1704 UT 23 April, 1969	12^h39^m	8°33′	182° ± 1°	8°47′ ± 1°	3° ± 2°
KSC, Japan						
K-9M-27	1215 UT 7 August, 1969	18^h3^m	31°15′	286° ± 1°	20° ± 1°	9° ± 1°
S-210-2	1200 UT 8 August, 1969	17^h52^m	31°15″	10° ± 2°	−13.0° ± 2°	39° ± 2°

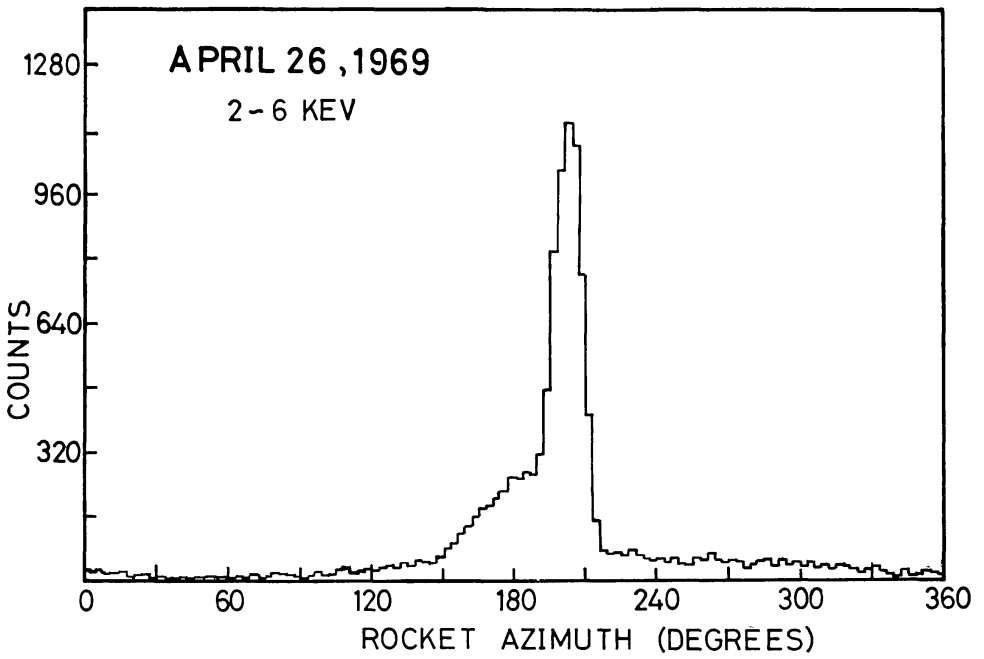

Fig. 2a.

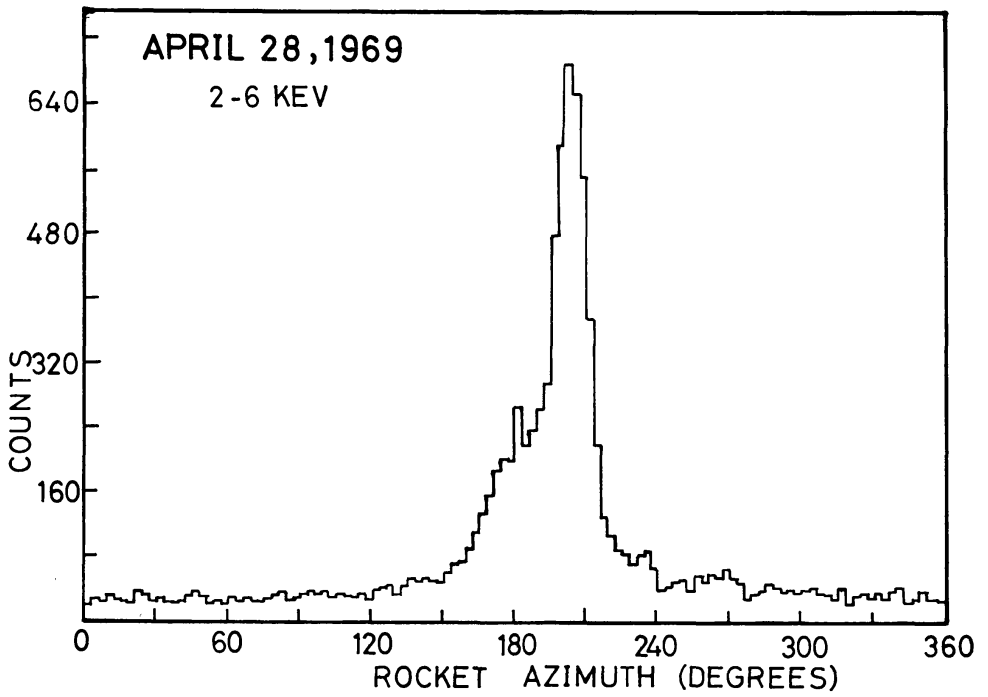

Fig. 2b.

Fig. 2a–b. The counting rate plotted as a function of rocket azimuth for the two rocket flights from TERLS on April 26 and April 28, 1969 for 2–6 keV energy windows.

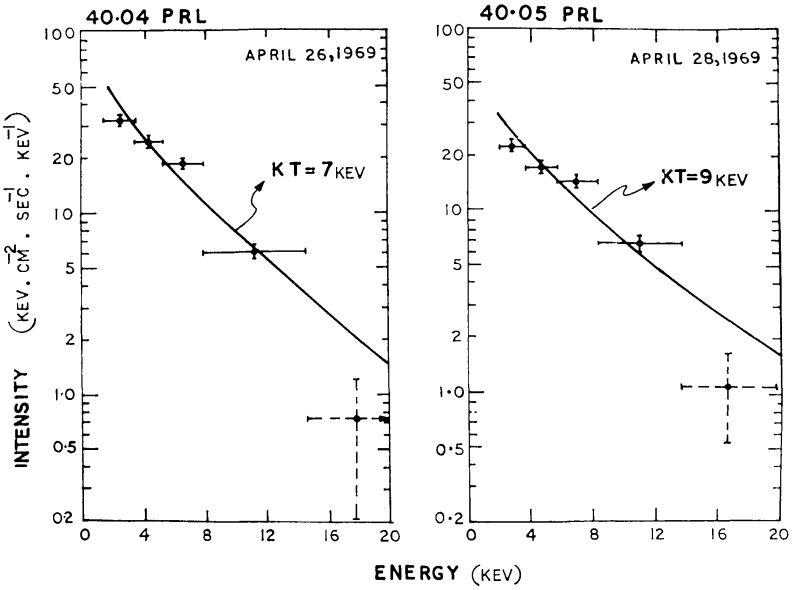

Fig. 3. The energy spectra of X-rays from SCO X-1 observed from TERLS on April 26 and April 28, 1969 respectively. The temperature fits to the data using a hot thin plasma model are also shown in the figure.

spectrum of the X-ray source is derived by convolving the observed counting rate and the pulse height spectrum with the efficiency and the energy resolution of the detector. Figure 3 shows the energy spectra obtained after the background correction for the rocket flights on April 26 and April 28, 1969, respectively conducted from TERLS, and Figure 4 shows the energy spectra for SCO X-1 obtained from KSC flights on August 7 and August 8, 1969 respectively. Notice that the difference in spectra observed on August 7 and 8 is quite apparent, in spite of the spectrum of the new source remaining constant.

5. Results and Discussion

Let us assume a simple model of a spherical hot cloud of radius r at a uniform temperature T and having a uniform density n. The free–free emission spectrum of such an X-ray source can be represented by an exponential spectrum

$$I_{ff}(\varepsilon) = 3.0 \times 10^{-15} \frac{n^2 r^3}{3d^2} g \exp\left(-\frac{\varepsilon}{kT}\right) (kT)^{-1/2} \text{ keV cm}^{-2} \text{ s}^{-1} \text{ keV}^{-1}, \quad (1)$$

where g is the Gaunt factor, r and d are in cm, n is in cm^{-3} and the photon energy ε and kT are in keV. Fitting the X-ray observations of SCO X-1 from the four rocket flights to an exponential spectrum, the parameters T and $n^2 r^3/3d^2$ have been estimated. In Table II these parameters are tabulated along with similar parameters calculated from the data obtained by the LRL group. The B magnitudes of SCO X-1, whenever available, have also been tabulated in the table. It is noticeable from the table, that the

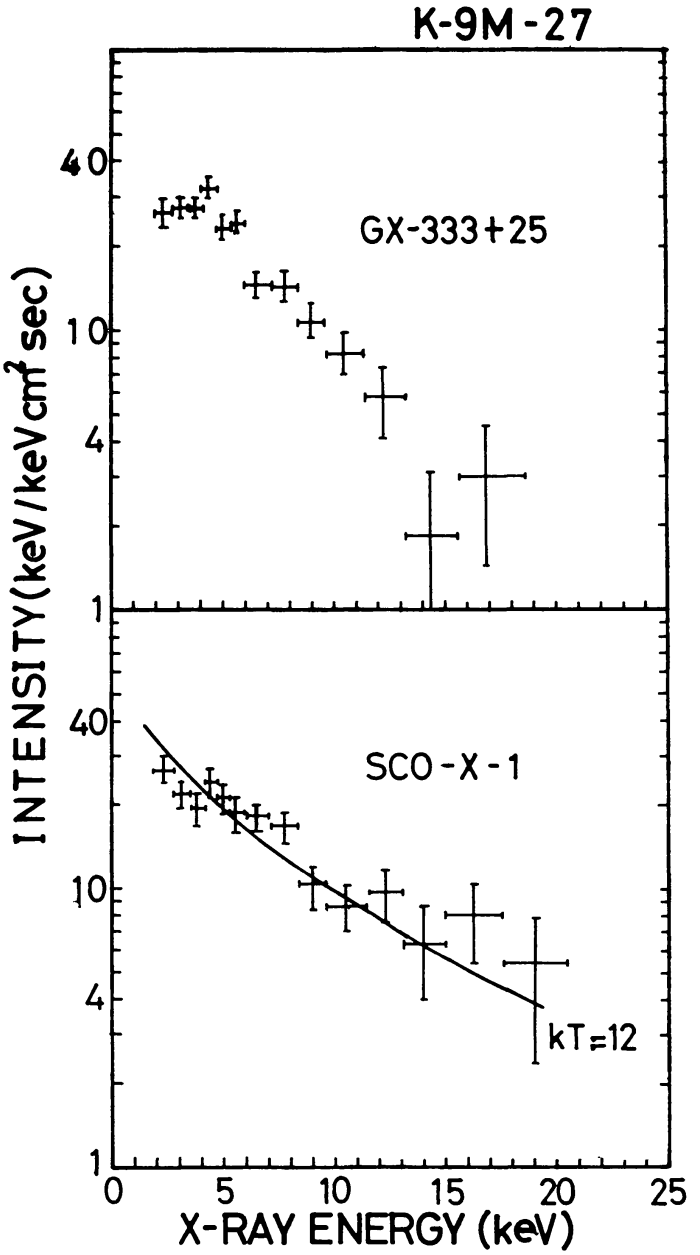

Fig. 4a.

effective temperature of SCO X-1 varies between $kT=4$ to 12 keV and the B magnitude varies between 12.5 mag. to 13.4 mag. The observation on August 7, 1969 indicates that the effective temperature of SCO X-1 was exceedingly high at that time and that the source was in the darkest phase of its optical luminosity (Ichimura and Noguchi, 1969).

The parameter $n^2r^3/3d^2$ for each observation has been calculated and is plotted as a function of kT in Figure 5. Figure 6 summarized all the available observations of simultaneous optical and X-ray measurements, and shows the relationship between kT and the optical intensity expressed by the blue magnitude B.

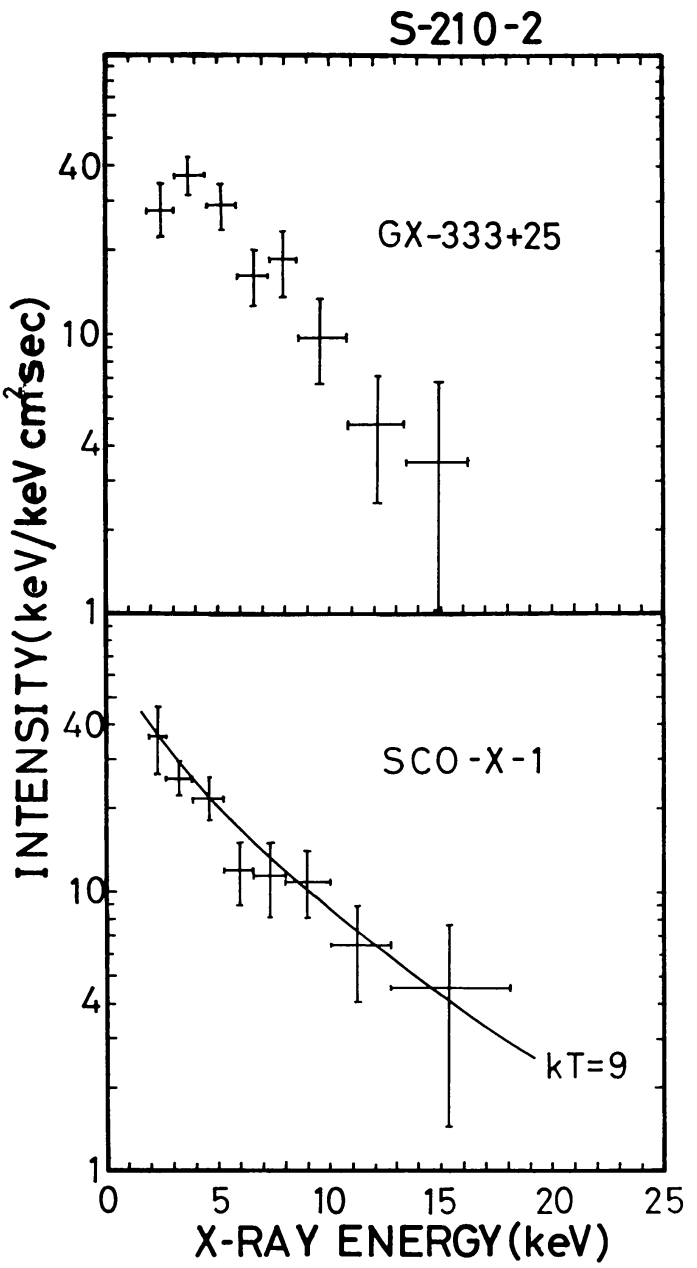

Fig. 4b.

Fig. 4a–b. The energy spectra of X-rays from SCO X-1 and GX333 + 25 observed from KSC on August 7 and August 8, 1969, respectively. The temperature fits to the data using a hot thin plasma model are also shown in the figure.

In spite of the large scatter of points plotted in Figures 5 and 6, the results indicate the existence of definitive relationships between T and B, and T and $n^2r^3/3d^2$ as shown by the dashed curves in the figures. This implies that the properties of the hot cloud are characterized by its temperature which, once specified, uniquely determines the physical nature of the cloud.

In the following we attempt to reproduce the spectra of SCO X-1 from the X-ray

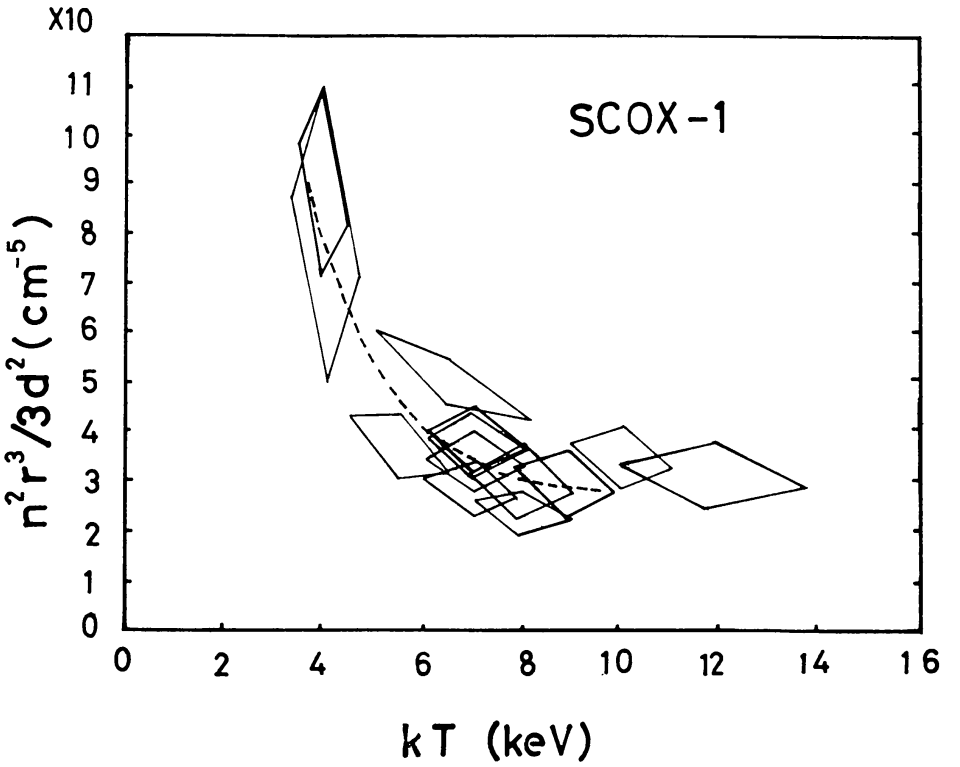

Fig. 5. The relation between the temperature kT and the value of $n^2r^2/3d^2$ of SCO X-1 compiled from the results obtained by rocket observations.

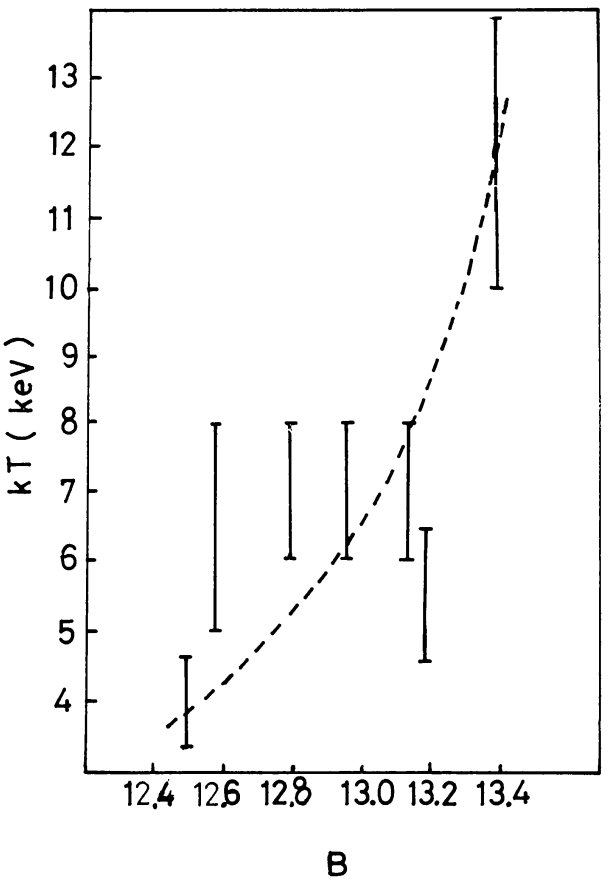

Fig. 6. The relation between the optical blue magnitude B and the temperature kT of SCO X-1 compiled from the results obtained by rocket observations.

TABLE II

Rocket observations of SCO X-1. LRL: observations by Lawrence Radiation Laboratory. TERLS observations by the collaborative group of Physical Research Laboratory and University of Tokyo at Thumba Equatorial Rocket Launching Station. KSC: observation by Osaka City University and University of Tokyo at Kagoshima Space Center. Effective temperatures have been determined in the energe range 2–20 keV taking the Gaunt factor into account.

Date		Effective temperature (kT in keV)	$n^2r^3/3d^2 \times 10^{-15}$ (cm^{-5})	B
1967, May 18	LRL	7 ± 1	37 ± 6	12.8
1967, Sept. 29	LRL	4 ± 0.7	80 ± 29	12.5
1968, May 9	LRL	7 ± 1	28 ± 6	13.15
1968, May 19	LRL	5.5 ± 1	38 ± 6	13.2
1969, April 26	TERLS	6.8 ± 1	31 ± 3	
1969, April 28	TERLS	8.6 ± 1.2	25 ± 3	
1969, Aug. 7	KSC	12 ± 2	30 ± 7	13.4
1969, Aug. 8	KSC	9 ± 1	28 ± 8	
1969, May 17	LRL	(8)	23 ± 5	13.19
1969, May 24	LRL	6.5 ± 1.5	50 ± 5	12.56

to the optical range for various values of T, using the relationship between the parameters T, B and $n^2r^3/3d^2$ compiled from observational results shown in Figures 5 and 6. The energy spectrum of the free–free emission generated by a semi-opaque plasma can be expressed by the approximate relation

$$I(\varepsilon) = \frac{1 - \exp(-\tau_{ff})}{\tau_{ff}} I_{ff}(\varepsilon). \tag{2}$$

The optical depth for free–free absorption, τ_{ff}, for small ε/kT is expressed by

$$\tau_{ff} = 7.7 \times 10^{-48} g (kT)^{-3/2} \varepsilon^{-2} n^2 r. \tag{3}$$

Fitting the result of the X-ray observation with the above relations, we can estimate n and r for an assumed distance. Let us assume that the interstellar absorption can be represented by an extinction curve with $A_V/(A_B - A_V) = 3$ and that the color excess of SCO X-1 is essentially constant; $B - V = 0.2$. We then correct the optical spectrum for various magnitudes of interstellar absorption. By fitting the corrected optical spectrum to the model spectrum, n^2r and A_V are determined. From $n^2r^3/3d^2$ and n^2r, n and r are calculated for an assigned distance to the source; 0.3 kpc and 1 kpc. The combination of B, T and $n^2r^3/3d^2$ used in the calculation, and the results of the calculation, are listed in Tables III(a) and III(b) respectively.

From these tables we conclude that the size and the density of the source are of the order of $10^8 \sim 10^9$ cm and $10^{16} \sim 10^{17}$ atoms cm^{-3} respectively, in agreement with previous investigations (Chodil *et al.*, 1968), and that for higher temperature the source is smaller and denser and vice versa. The resultant A_V is somewhat larger than is expected for the assumed distance. This difference may be due to the fact that the

TABLE III(a)

Physical parameters of SCO X-1 (a), and the calculated results as an isothermal hot cloud model (no correction for electron scattering), (b)

kT (keV)	$n^2r^3/3d^2$ (cm^{-5})	B (mag.)
4	8×10^{16}	12.5
6	4×10^{16}	12.9
8	3×10^{16}	13.1
10	3×10^{16}	13.3
12	3×10^{16}	13.4

TABLE III(b)

kT (kev)	A_V (mag)	$d = 0.3$ kpc			$d = 1.0$ kpc		
		r(cm)	n(cm^{-3})	τ_{es}	r(cm)	n(cm^{-3})	τ_{es}
4	1.2	2.9×10^8	9.1×10^{16}	17.6	9.7×10^8	5.0×10^{16}	32.4
6	1.1	2.2×10^8	9.7×10^{16}	14.3	7.4×10^8	5.3×10^{16}	26.3
8	1.0	1.4×10^8	1.6×10^{17}	15.2	4.8×10^8	8.8×10^{16}	27.9
10	1.0	1.2×10^8	2.1×10^{17}	16.8	4.0×10^8	1.2×10^{17}	30.8
12	1.0	1.0×10^8	2.7×10^{17}	18.1	3.4×10^8	1.5×10^{17}	33.2

distance is a little larger than assumed or that a part of the extinction is due to a circumstellar dust cloud.

In the above estimate the photon is considered to exchange energy with the plasma by free–free absorption. In fact, however, the photons produced in the cloud are scattered by electrons many times before they come to the surface of the cloud, which may result in a distortion of the photon spectrum. Analytical treatment of the electron scattering under such a condition is complicated. Chodil *et al.* (1968) used a conventional diffusion theory to take this effect into consideration.

Loh and Garmire (1970) treated the problem by means of a Monte Carlo calculation to estimate the distortion of the spectrum. It was shown by taking the distortion into account that the apparent temperature of the cloud, T, determined from the X-ray spectrum in terms of the free–free emission mechanism, appears to be significantly higher than the temperature of the source, T_0. They worked out model spectra from the infrared to the X-ray range for a limited number of combinations of the following parameters; T_0, n, r.

The results of Loh and Garmire were simulated by the following formulae:

$$\begin{aligned} T &= T_0 (1 + 0.00475\, \tau_{es}^{2.5}), \\ I &= \frac{1 - \exp(\tau_a)}{\tau_a} I_{ff}(T), \\ \tau_a &= (3 [\tau_{ff}(T_0)]^3\, \tau_{es})^{1/4}\, r, \\ \tau_{es} &= \sigma_T n r, \end{aligned} \tag{4}$$

where σ_T represents the Thomson scattering cross-section. Assuming that these expressions are valid for wider ranges of T, n and r, we have extrapolated the Loh-Garmire calculations and produced modified model spectra for various combinations of the parameters. The results thus calculated are listed in Table IV.

We have fitted the modified spectrum to the observed spectrum in the X-ray range, and the optical range corrected for interstellar absorption, as was done for the free–free emission spectrum. We obtain lower temperatures compared to those we obtained using the free–free emission spectrum; $kT=2\sim6$ keV instead of $4\sim12$ keV. This means that the cloud would be a little larger, by a factor of about four and thinner by a factor of about seven than that of the previous estimation. It should, however, be remarked that the estimates using the free–free emission spectrum are essentially valid, except for numerical factors until a more precise calculation taking into account the effect of the electron scattering is made.

It should be emphasized that the size of the source is very small, comparable to or smaller than the size of a white dwarf. It may also be noted that this size is consistent with the distance in which a gas of this temperature is confined by the gravitational force of a central body of one solar mass. The variation of size with temperature is consistent with the gravitational confinement of the hot plasma. The change in the density is not proportional to r^{-3}, thus indicating the accretion of matter in the bright phase.

Satellite measurements of the X-ray intensity of SCO X-1 on two Vela 5 satellites were reported for two periods of approximately 4 h each (Evans *et al.*, 1970). In one of the periods simultaneous optical observations were made and an optical flare was observed. Another period contained large and rapid changes in the X-ray intensity. Assuming that the thin hot cloud model is applicable similarly in the flare period, we estimated n^2r^3 and kT for the pre-optical-flare period (August 2) and for the period of sudden X-ray increases or X-ray flares (October 17) from the published data. We plotted the results on the diagrams $n^2r^3/3d^2$ versus kT and B versus kT as are shown in Figures 7 and 8. For the X-ray flare period of October 17 optical data are lacking. Assuming that the optical flare coincides with the X-ray flare and that the optical flare appears when SCO X-1 is in its bright phase ($B\lesssim12.6$), we obtain the square representing a flare on the B versus kT diagram. The results from OSO III by Hudson *et al.* (1970) are also plotted in the same figures.

We tentatively interpret the presently available data on the variation of SCO X-1 as follows. There are two modes of variations, one being the non-flare (quiet) variation and another being the flare-type variation; and the source in the two modes behaves differently on the diagrams.

Summarizing for the quiet mode we conclude as follows:

(1) The X-ray source SCO X-1 is well characterized by its temperature. Simple relationships exist between the temperature, the density and the size of the source.

(2) Simultaneous optical and X-ray observations show that the SCO X-1 source is characterized by a temperature of about $10^7\sim10^8$ K, a density of about $10^{16}\sim10^{17}$ cm^{-3} and a radius of about $10^8\sim10^9$ cm, respectively.

TABLE IV

Physical parameters of SCO X-1 calculated as an isothermal hot cloud model (corrected for electron scattering)

kT(keV)	A_V(mag.)	$d = 0.3$ kpc				$d = 1.0$ kpc			
		kT_0(keV)	r(cm)	n(cm^{-3})	τ_{es}	kT_0(keV)	r(cm)	n(cm^{-3})	τ_{es}
4	1.1	1.5	9.3×10^8	1.6×10^{16}	9.9	0.9	4.8×10^9	4.5×10^{15}	14.5
6	0.9	2.7	5.6×10^8	2.4×10^{16}	9.1	1.5	3.0×10^9	6.3×10^{15}	12.9
8	0.9	3.7	4.3×10^8	3.1×10^{16}	8.9	2.1	2.4×10^9	8.0×10^{15}	12.7
10	0.9	4.4	3.8×10^8	3.7×10^{16}	9.4	2.5	2.1×10^9	9.7×10^{15}	13.5
12	1.0	4.8	3.5×10^8	4.3×10^{16}	9.9	2.6	1.9×10^9	1.1×10^{16}	14.0

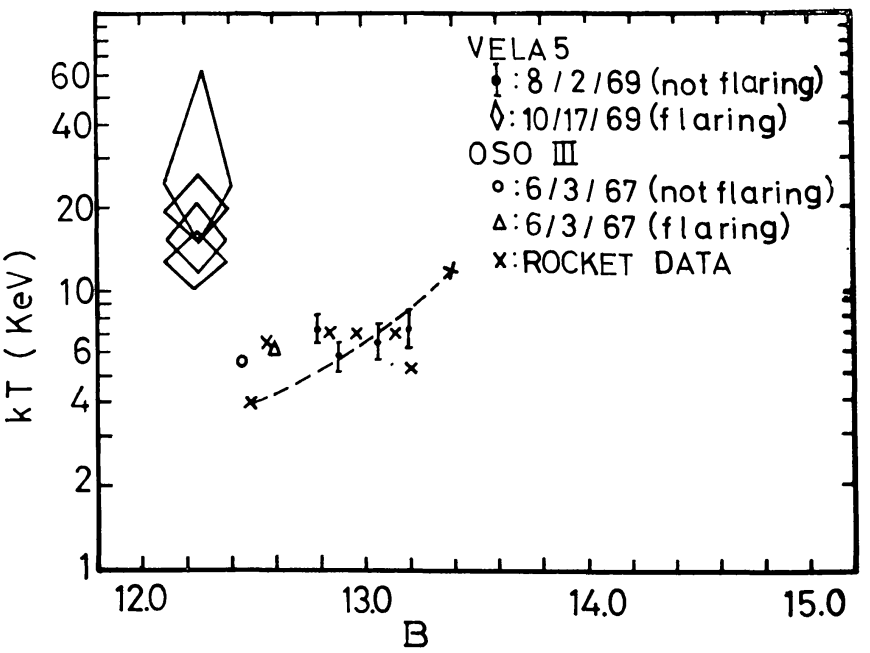

Fig. 7. The relation between the temperature kT and the values of $n^2r^2/3d^2$ of SCO X-1 compiled from the satellite data. For comparison, the data obtained by rockets are shown by symbol X. The intensities obtained by OSO-III seem to be 60% larger than the others. This figure shows clearly that there are two modes of variation of SCO X-1, not flaring and flaring modes.

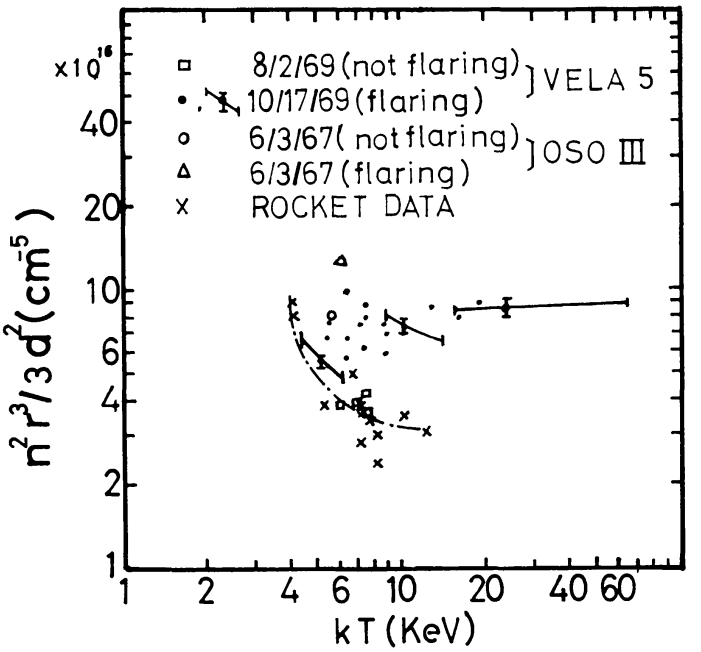

Fig. 8. The relation between the optical blue magnitude B and the temperature kT of SCO X-1 compiled from the satellite data. For comparison, the data obtained by rockets are shown by symbol X.

(3) The size of the source is very small, comparable to or smaller than the size of a white dwarf. The source size of $r = 10^8 \sim 10^9$ cm is consistent with a distance in which the gas of this temperature is confined by the gravitational force of a central body of approximately solar mass. The size is inversely correlated with the temperature, being in agreement with the gravitational confinement of the plasma.

Acknowledgements

The Nike-Apache rockets for the experiments were made available under the NASA-INCOSPAR agreement, for which the authors are grateful to Dr V. A. Sarabhai. The authors are also indebted to Messrs H. G. S. Murthy, A. P. J. Abdul Kalam, R. Aravamudan, and their associates for help in launching the rockets from TERLS. The work done in India was supported by the funds from the Department of Atomic Energy, Government of India.

The authors thank Professor K. Osawa and the staff of Okayama Astrophysical Observatory for their continuous interest and collaboration in the simultaneous observations of SCO X-1. They also thank the personnel of the Institute of Space and Aeronautical Science for support of our rocket experiments, and we are indebted to M. Kaneko, K. Mihara and F. Yamamoto who contributed the experiments by technical assistance. The authors are grateful to Professor G. Garmire of California Institute of Technology for discussion and for showing us his unpublished calculations.

Added in proof: It is interesting to note that the result of LRL flight of 1968, May 15 ($B = 12.47$; $kT = 12 \pm 4$ keV; Grader *et al.*, *Astrophys. J.* **159** (1970) 201), which took place only a few minutes before an optical flare, is consistent with the flaring mode indicated in Figure 7.

References

Burginyon, G. A., Grader, R. J., Hill, R. W., Hiltner, W. A., Mannery, E. J., Price, R. E., Rodrigues, R., Seward, E. D., and Swift, C. D.: 1970, *Astrophys. J.* **161**, 987.

Chodil, G., Mark, H., Rodrigues, R., Seward, F. D., Swift, C. D., Turiel, I., Hiltner, W. A., Wallerstein, G., and Mannery, E. J.: 1968, *Astrophys. J.* **154**, 645.

Conner, J. P., Evans, W. P., and Belian, R. D.: 1969, *Astrophys. J.* **157**, L157.

Evans, W. D., Belian, R. D., Conner, J. P., Strong, I. B., Hiltner, W. A., and Kunkel, W. E.: 1970, *Astrophys. J.* **162**, L115.

Giacconi, R., Gursky, U., Paolini, F., and Rossi, B.: 1962, *Phys. Rev. Letters* **9**, 439.

Hiltner, W. A. and Mook, D. E.: 1970, *Ann. Rev. Astron. Astrophys.* **8**, 139.

Hudson, H., Peterson, L. E., and Schwartz, D. A.: 1970, *Astrophys. J.* **159**, L51.

Ichimura, K., and Noguchi, T.: 1969, *Tokyo Astron. Bull.*, second series, No. 195, 2275.

Kitamura, T., Matsuoka, M., Miyamoto, S., Nakagawa, M., Oda, M., Ogawara, Y., and Takagishi, K.: 1969, *Nature* **224**, 784.

Loh, E. D. and Garmire, G. A.: 1970, private communication.

Neugebauer, G., Oke, J. B., Becklin, E., and Garmire, G. A.: 1969, *Astrophys. J.* **155**, 1.

Sandage, A. R., Osmer, P., Giacconi, R., Gorenstein, P., Gursky, H., Waters, J., Bradt, H., Garmire, G., Sreekantan, B. V., Oda, M., Osawa, K., and Jugaku, J.: 1966, *Astrophys. J.* **146**, 316.